



Article citation info:

Fang Y, Wang Y, Sha J, Gu T, Zhang H, A mechanism reliability analysis method considering environmental influence and failure modes' correlation: a case study of rifle automaton Eksploatacja i Niezawodność – Maintenance and Reliability 2023: 25(2) <http://doi.org/10.17531/ein/166145>

A mechanism reliability analysis method considering environmental influence and failure modes' correlation: a case study of rifle automaton

Indexed by:
 Web of Science Group

Yi-chuan Fang^a, Yong-juan Wang^{a, *}, Jin-long Sha^b, Tong-guang Gu^a, He Zhang^a

^a School of Mechanical Engineering, Nanjing University of Science and Technology, Nanjing, Jiangsu Province, China

^b NO.208 Research Institute of China Ordnance Industries, Beijing China

Highlights


- The method is applicable to multi-body mechanisms without available analytical solutions.
- Environmental influence is quantified and incorporated into the reliability model.
- Copula function is employed to represent related structures among multiple failure modes.
- The proposed method is more reasonable, practical and precise.

Abstract

In order to overcome the challenge of quantifying the influence of environmental conditions and the coexistence of multiple failure modes involved in mechanism reliability modelling under different environments. In this paper, we propose a method for the analysis of mechanism reliability that takes into account the influence of environmental factors and failure modes' correlation, quantifies the influence of environmental factors as the random distribution and degradation path of parameters, and derives the Copula description of failure mode correlation from the historical data of environmental experiments. On the basis of the discrete mechanism dynamics model, the output parameters of the characteristic points are calculated, and the failure rate of each failure mode is calculated based on the failure criterion and the performance margin theory. Additionally, the dynamic change pattern of the mechanism reliability is compared with the Kaplan-Meier estimation of the corresponding environmental test history data to assess the validity of the calculation results. The reliability modelling problem of a motion mechanism of an automatic rifle automaton in a high and low temperature environment is applied to the method, and the reliability calculation results are close to those of Kaplan-Meier estimation of the test history data, and all are within the upper and lower bounds given by the reliability boundary theory, demonstrating the method's validity.

Keywords

mechanism reliability, environmental influence, failure modes' correlation, copula function, Kaplan-Meier estimation, rifle automaton

This is an open access article under the CC BY license (<https://creativecommons.org/licenses/by/4.0/>) 

1. Introduction

1.1 Literature review

The mechanism reliability problem can be divided into the reliability problem related to the load-bearing capacity and the reliability problem related to the motion function [8], the former is generally attributed to the reliability problem of mechanical structure parts, and mature methods are available; the latter is

vastly distinct from the general strength reliability problem, which is the main topic of this paper. The reliability of the motion performance of a mechanism is its ability to perform the specified motion function under specified conditions and within specified time [38]. In recent years, as the frequency of failures associated with the motion performance of a mechanism has increased [5,16,28,31], the topic of a motion reliability has

(*) Corresponding author

E-mail addresses: Y. Fang (ORCID: 0000-0001-7119-6360) smefangyichuan@njust.edu.cn, Y. Wang (ORCID: 0000-0002-0683-7587) 13951643935@139.com, J. Sha, 1371319231@qq.com, T. Gu 524737798@qq.com, H. Zhang zh54529443@163.com

received a growing amount of attention. The motion performance reliability of a mechanism essentially describes the relationship between the performance parameter of the system and the safety boundary. The performance parameter of a system is a comprehensive performance of its internal subsystems at different levels. Due to the growing complexity of the structure and function of mechanisms, the independent and incidental factors that induce mechanism failure are relatively decreased, and the mechanism has multiple failure modes due to the variance of working time, working stage and working environment. Hence, the problems of degradation of performance parameters, random distribution of loads and description of failure modes further aggravate the complexity of mechanism reliability analysis.

Mechanism reliability theory has spawned numerous subfields, one of which is the study of mechanism motion accuracy, i.e., the examination of the discrepancy between the ideal and real output parameters of the mechanism. Lee and Gilmore [15] proposed a probabilistic modelling approach to determine the mean and variance of velocity and acceleration within a randomly defined kinematic chain of planar pin connections, considering the effects of linkage length tolerance, radial clearance, and pin center position. Qing et al. [19] developed a mechanism motion reliability model for the locking mechanism of a planetary probe and evaluated the dynamic characteristics of the mechanism in three aspects: static torque margin (after deployment), driving torque (during deployment), and torque power (energy). Wu et al. used a rigid-body model to identify the status of the mechanism based on its health index and to generate a large sample of failure times. Then Kaplan-Meier estimation was performed to evaluate the mechanism reliability of a bistable compliant mechanism [29] and a crank-slider mechanism [30]. Wang et al. [20] employed reliability analysis methods to assess the positioning accuracy of the robot end-effector, as well as linear regression and iterative Taylor series methods to deal with the limit states in reliability calculations. Zhang et al. [36] investigated the robot mechanism with random dimensions and joint angles, the kinematic reliability is determined by the probability of the actual position of the end-effector falling into a specific tolerance range centered on the target position, and then the saddle-point approximation is applied to calculate the kinematic reliability.

When it comes to degradation of mechanism parameters, random shocks, and environmental changes, it is more convenient to treat the dynamic changes in mechanism reliability as a stochastic process. Huang et al. [33] studied systems subject to both internal failures and external shocks, and external shocks were modeled using the Poisson process and the reliability of the system was calculated based on survival signature theory. Rafiee et al. [24] established a categorization technique for external shocks in system reliability analysis and evaluated the impact of generalized hybrid shock model for systems with competing failure modes. Shen et al. [26] investigated system degradation affected by both continuous degradation and random shocks, and determined the reliability of tandem systems in a recursive manner by examining the correlation between degradation process and random shocks. For the quantification of environmental factors in reliability analysis, Sidum et al. [2] used Bayesian networks to predict the effect of environmental factors on corrosion rate due to seawater pH, seawater temperature, and seawater salinity in order to assess the reliability of offshore systems, and then established the limit state function corresponding to each failure mode of the mechanism under microbial corrosion. Mahdi et al. [22] used a stochastic process to simulate the environmental factors brought by external shock and the aging of the system, and also provided a general method for system reliability assessment using the survival signature theory and a maintenance strategy for multi-component systems subject to the external environmental influence. Zheng et al. [37] established a proportional risk model with degradation trend and environmental factors as covariates. A Wiener process is firstly applied to describe the degradation path, and then a proportional risk model is established with the degradation path and temperature as covariates to finally derive the closed form of reliability by Taylor approximation.

Traditional methods for failure correlation analysis of mechanical systems [4,32,34] are usually based on correlation coefficients. However, only linear correlation coefficients can be used to describe the relationship between variables, which cannot be applied to nonlinear situations, and the computational effort will increase dramatically as the number of failure modes increases. To minimize the running duration of Monte Carlo

simulations, Stern et al. [27] proposed an approximate framework (implemented by support vector machines and an alternative model based on logistic regression) for correlation quantification of samples using machine learning-based classifiers. Limit methods and their improvements [21] can give upper and lower bounds on the reliability of a system when there are multiple failure modes, but such methods are only applicable to series systems and are computationally intensive. Copula functions are useful tools for describing correlations between variables and have been widely used in the field of reliability modelling, such as Copula functions combined with evidence theory [12], Copula functions applied to multi-state k-out-of-n systems [18] and Copula functions applied to competing failure-related systems subject to degradation and shocks [10].

1.2 Current problems

The motion reliability analysis of a mechanism is mainly focused on kinematic analysis, and the research objects are predominantly mechanisms with more mature motion characteristics, whereas the problems of reliability modelling of complex mechanisms and their dynamics are rarely addressed. The majority of current research treats the effect of environmental conditions as a stochastic process, which undermines the influence of environmental factors and is insufficient for the description of engineering practice. When there are multiple failure modes in the mechanism, the traditional method without considering the failure modes' correlation or only introducing linear correlation coefficients for correlation description is not applicable, and using Copula function is a better way to handle it, but it is rarely applied in the reliability modelling of mechanisms with multiple failure modes.

1.3 Main contributions

For the reliability modelling problem of mechanism in a specific environment, this paper proposes a general approach to deal with such engineering problems, and the main contributions include the following three aspects:

1) The reliability modelling of the mechanism does not adopt the traditional DPM (Direct Probabilistic Method) method to avoid the situation that the mechanism performance output cannot be applied when no analytical formula is available.

Instead, a discrete dynamics model is used to calculate the output parameters of each characteristic point, and the dynamic change law of the mechanism reliability is given according to the failure criterion and performance margin.

2) Considering the influence of environmental factors in the mechanism reliability modelling, attributing the essence of environmental factors introduced into the system to the degradation path of the mechanism parameters and the change of the random distribution of the parameters, thus quantifying the influence of environmental factors on the mechanism reliability.

3) When there are multiple failure modes in the mechanism, the assumption of independence of failure modes is not applicable, and Copula function is introduced as a tool to quantify the correlation of failure modes in the mechanism, so as to avoid the problem of poor flexibility caused by using only linear correlation coefficients and the problem of computational burden brought by multiple integrals.

2. Research methodology

The flow chart of the mechanism reliability analysis research method considering the influence of environmental factors and failure modes' correlation is shown in Figure 1.

The main body of the flow chart is the traditional model based on mechanism dynamics to calculate the failure probability of mechanism with multi failure modes. The environmental factors are introduced into the discrete mechanism dynamics model in the form of parameter degradation path and parameter random distribution. The Copula description of the failure modes' correlation and the influence of environmental factors are derived from the historical data of environmental experiments, and the final reliability calculation results can be compared with the Kaplan-Meier estimation of the experimental censored data to evaluate the calculation accuracy of the model.

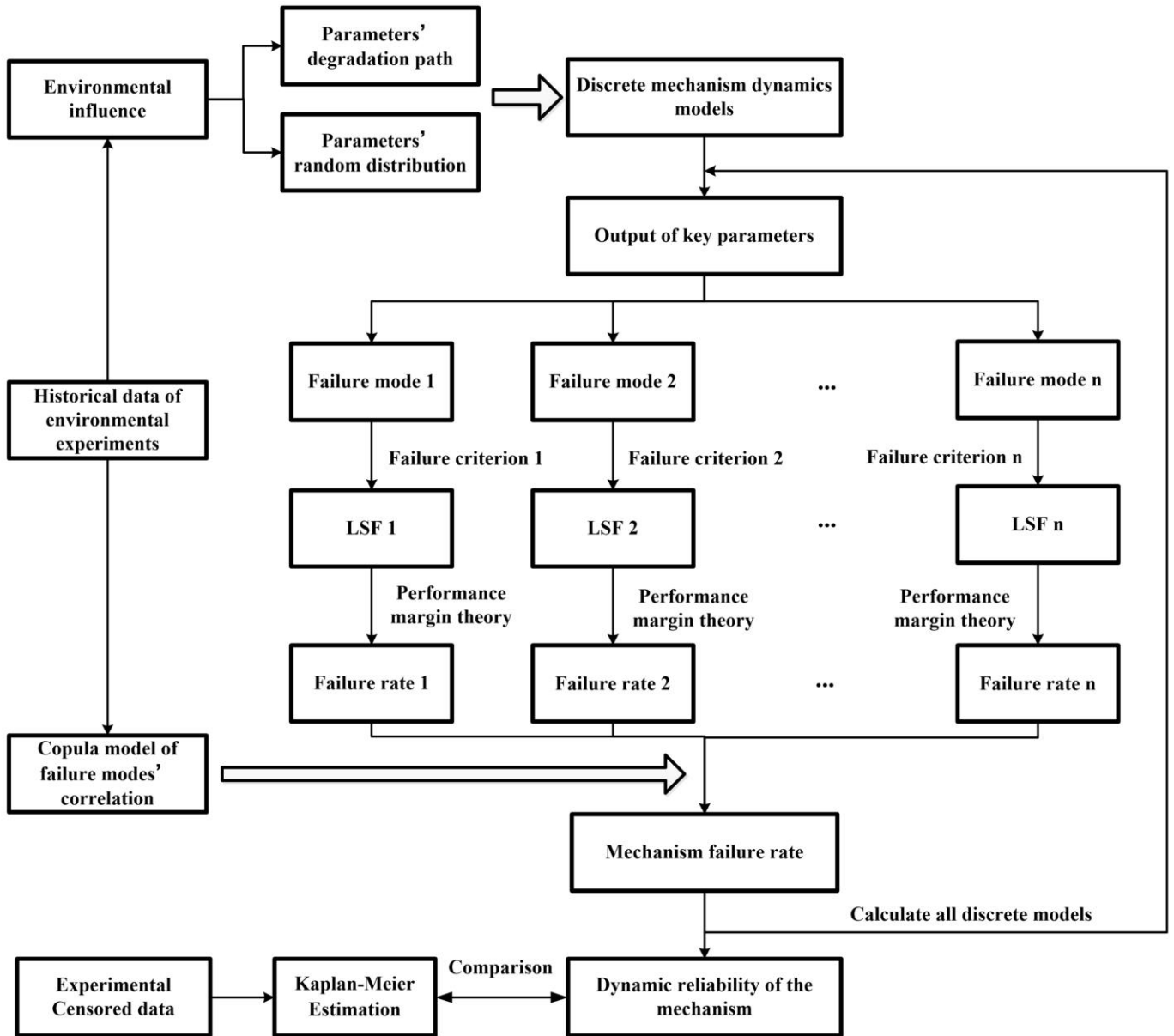


Fig.1. The flow chart of the proposed methodology.

2.1 Modelling of mechanism dynamics with impact

For impact transmission is prevalent in all types of motion mechanisms, and the impact process is sensitive to external influences, thus adding more uncertainty to the system. The essence of modelling the dynamics of a mechanism with impact process is to solve the generalized velocity of each part in the mechanism based on the coefficient of restitution according to the normal kinematic relationship between the impact points (or impact planes). During the impact process, the displacement of the member at the impact point (or impact plane) remains constant and the velocity changes abruptly. After the impact, a Lagrange multiplier must be introduced to the impact point to be consistent with the displacement constraint, which is related

to the impact impulse that causes the abrupt change in velocity.

The dynamical equations of the system before the impact can be expressed as

$$\begin{bmatrix} M & \Phi_q^T \\ \Phi_q & 0 \end{bmatrix} \begin{bmatrix} \ddot{q} \\ \lambda \end{bmatrix} = \begin{bmatrix} Q^* + Q^e \\ \gamma \end{bmatrix} \quad (1)$$

where M is the generalized mass matrix of the pre-impact system, Φ_q is the Jacobi matrix of the pre-impact system constraints, λ denotes the binding vector, Q^* is the velocity quadratic term obtained by deriving the kinetic energy twice with respect to time, Q^e is the external force vector, γ is the term at the right end of the acceleration constraint equation, and q is the generalized coordinate array of the system.

The kinetic equation for the impact phase is:

$$\begin{bmatrix} M & \Phi_q^T & \frac{\partial s_n^T}{\partial q} \\ \Phi_q & 0 & 0 \\ \frac{\partial s_n}{\partial q} & 0 & 0 \end{bmatrix} \begin{bmatrix} \Delta \dot{q} \\ I^\lambda \\ -p \end{bmatrix} = \begin{bmatrix} 0 \\ 0 \\ -(1+e) \frac{\partial s_n^T}{\partial q} \dot{q}(t^-) \end{bmatrix} \quad (2)$$

where s_n is the shortest normal distance vector array between the impact points, $\Delta \dot{q}$ is the change of the generalized velocity due to the impact, I^λ is the binding force impulse due to the impact, p denotes the impact force impulse, e is the impact recovery factor, t is the impact moment, and $\dot{q}(t^-)$ is the generalized velocity of the system before the impact.

The generalized velocity $\dot{q}(t^+)$ of the post-impact system is then derived as

$$\dot{q}(t^+) = \dot{q}(t^-) + \Delta \dot{q} \quad (3)$$

2.2 Discretization of the dynamics model considering environmental factors

Environmental factors incorporated into the model are mainly represented by parameters with random distribution and parameters with degradation path. Due to the strong nonlinearity of the impact process, the mechanism dynamics model needs to be discretized by impact time nodes. Let the working process of the mechanism can be divided into m time periods, and each time period consists of n time points, then the working time matrix of the mechanism can be expressed as:

$$T = \begin{bmatrix} t_{11} & t_{12} & \dots & t_{1(n-1)} & t_{1n} \\ \dots & \dots & \dots & \dots & \dots \\ t_{i1} & t_{i2} & \dots & t_{i(n-1)} & t_{in} \\ \dots & \dots & \dots & \dots & \dots \\ t_{m1} & t_{m2} & \dots & t_{m(n-1)} & t_{mn} \end{bmatrix} = \begin{pmatrix} T_1 \\ \dots \\ T_i \\ \dots \\ T_m \end{pmatrix}_m \quad (4)$$

where t_{ir} denotes the r^{th} ($r = 1, 2, \dots, n$) time point of the i^{th} ($i = 1, 2, \dots, m$) time period.

$$T_i = [t_{i1}, t_{i2}, \dots, t_{i(n-1)}, t_{in}] \quad (5)$$

Each period consists of time points evenly distributed along the time axis.

$$\Delta t = t_{ir} - t_{i(r-1)} = \frac{t_{in}}{n} \quad (r, i = 1, 2, \dots, n) \quad (6)$$

The randomness and degradation path of the input parameters are described by the variation of the mean and standard deviation. During this period, the mean and standard deviation are assumed to be:

$$\mu_i = \begin{bmatrix} \mu_{i1}^{(1)} & \mu_{i2}^{(1)} & \dots & \mu_{i(n-1)}^{(1)} & \mu_{in}^{(1)} \\ \dots & \dots & \dots & \dots & \dots \\ \mu_{i1}^{(u)} & \mu_{i2}^{(u)} & \dots & \mu_{i(n-1)}^{(u)} & \mu_{in}^{(u)} \\ \dots & \dots & \dots & \dots & \dots \\ \mu_{i1}^{(p)} & \mu_{i2}^{(p)} & \dots & \mu_{i(n-1)}^{(p)} & \mu_{in}^{(p)} \end{bmatrix}_{p \times n} \sigma_i \quad (7)$$

$$= \begin{bmatrix} \sigma_{i1}^{(1)} & \sigma_{i2}^{(1)} & \dots & \sigma_{i(n-1)}^{(1)} & \sigma_{in}^{(1)} \\ \dots & \dots & \dots & \dots & \dots \\ \sigma_{i1}^{(u)} & \sigma_{i2}^{(u)} & \dots & \sigma_{i(n-1)}^{(u)} & \sigma_{in}^{(u)} \\ \dots & \dots & \dots & \dots & \dots \\ \sigma_{i1}^{(p)} & \sigma_{i2}^{(p)} & \dots & \sigma_{i(n-1)}^{(p)} & \sigma_{in}^{(p)} \end{bmatrix}_{p \times n}$$

The degradation path of parameters during the i^{th} time period is described by the degradation function D_i .

$$D_i(\mu_i, \sigma_i, T_i) = 0 \quad (8)$$

The dynamic equation of the output in the i^{th} time period can be written as:

$$x(T_i, \mu_i, \sigma_i) = 0 \quad (i = 1, 2, \dots, m) \quad (9)$$

The dynamic output S_i obtained from the kinetic equations with parameter randomness can be expressed as:

$$S_i = \begin{bmatrix} S_{i1}^{(1)} & S_{i2}^{(1)} & \dots & S_{i(n-1)}^{(1)} & S_{in}^{(1)} \\ \dots & \dots & \dots & \dots & \dots \\ S_{i1}^{(j)} & S_{i2}^{(j)} & \dots & S_{i(n-1)}^{(j)} & S_{in}^{(j)} \\ \dots & \dots & \dots & \dots & \dots \\ S_{i1}^{(q)} & S_{i2}^{(q)} & \dots & S_{i(n-1)}^{(q)} & S_{in}^{(q)} \end{bmatrix}_{q \times n} \quad (10)$$

where q denotes the number of output parameters, i.e. the number of generalized coordinates.

The ideal dynamic output calculated from the dynamic equation in the i^{th} time period can be expressed as:

$$S_i^* = s(T_i, \varphi_i, \mu_i = \text{constant}, \sigma_i = 0) \quad (11)$$

$$= \begin{bmatrix} S_{i1}^{(1)*} & S_{i2}^{(1)*} & \dots & S_{i(n-1)}^{(1)*} & S_{in}^{(1)*} \\ \dots & \dots & \dots & \dots & \dots \\ S_{i1}^{(j)*} & S_{i2}^{(j)*} & \dots & S_{i(n-1)}^{(j)*} & S_{in}^{(j)*} \\ \dots & \dots & \dots & \dots & \dots \\ S_{i1}^{(q)*} & S_{i2}^{(q)*} & \dots & S_{i(n-1)}^{(q)*} & S_{in}^{(q)*} \end{bmatrix}_{q \times n}$$

where q denotes the number of output parameters, m denotes the number of periods, and n denotes the number of time points in each time period. The computation time is proportional to $q \cdot m \cdot n$. For highly reliable or very long-lived products, this leads to a computational explosion. To simplify the calculation, it can be considered that some of the variable parameters within each cycle are constant, considering the relatively slow degradation process of mechanical products and the relatively short length of each cycle.

2.3 Mechanism reliability modelling based on margin equation

Kang [14] proposed the basic principles of reliability science

and established the corresponding reliability theoretical discourses. Margin equation is:

$$\mathbf{M} = G(\mathbf{P}, \mathbf{P}_{th}) > 0 \quad (12)$$

where \mathbf{M} is the performance margin vector, \mathbf{P} represents the performance parameter vector, \mathbf{P}_{th} identifies the performance threshold vector. When the vector of performance parameters does not exceed its critical value, i.e. $\mathbf{M} > 0$, the system is able to perform reliably.

For a specific mechanism, assuming that its designed value of the performance parameter in state J is P_j , and subject to various uncertainties, the actual performance parameter of the mechanism is P_j^r , the performance parameter error δ can be written as:

$$\delta = |P_j^r - P_j| \quad (13)$$

The maximum value of the performance parameter error is set to ε . The performance margin equation for the mechanism can be obtained as:

$$\mathbf{M} = \frac{\varepsilon - \delta}{\varepsilon} \quad (14)$$

In practical engineering problems, the performance margin is defined in terms of both the random uncertainty under internal and external environment and the cognitive uncertainty in the judgment of the allowable error of the performance parameters due to the limitation of the cognitive level, denoted as $\tilde{\mathbf{M}}$. The system can be considered reliable by quantifying $\tilde{\mathbf{M}}$ and ensuring that its value is always greater than 0. Therefore, the mechanism reliability model based on the performance margin is:

$$R_j = P(\tilde{\mathbf{M}} > 0) = P\left(\frac{\varepsilon - |P_j^r - P_j|}{\varepsilon} > 0\right) \quad (15)$$

2.4 Copula description of failure mode correlation

2.4.1 Selection of Copula function and its parameter estimation

The commonly used metrics for selecting Copula functions are divided into two categories [21], one is the correlation coefficient metric represented by Kendall correlation coefficient and Spearman correlation coefficient, and the other is the fitting parameter metric represented by squared Euclidean distance. In this paper, the optimal Copula function is selected by calculating the squared Euclidean distance, and the basic procedure is as follows:

(1) Sample points are generated based on the failure rate distribution function of each failure mode. Binary frequency

histograms of the two failure modes are drawn, and the initial Copula functions are selected according to the characteristics of the histograms. The commonly used Copula functions [6,17,35] include normal Copula function, t-Copula function and Archimedean Copula function, and the binary distribution functions and parameter ranges of various Copula functions are shown in Table 1.

Table 1. Binary distribution functions and parameter ranges of various Copula functions.

Copulas	binary distribution functions	parameter ranges
Gaussian	$\Phi_\rho(\Phi^{-1}(u), \Phi^{-1}(v))$	$\rho \in (-1,1)$
t	$t_{\rho,k}(t_k^{-1}(u), t_k^{-1}(v))$	$\rho \in (-1,1)$
Gumbel	$\exp(-[(-\ln u)^\alpha + (-\ln v)^\alpha]^{1/\alpha})$	$\alpha \in (1, +\infty)$
Frank	$-\frac{1}{\alpha} \ln \left(1 + \frac{(e^{-\alpha u} - 1)(e^{-\alpha v} - 1)}{e^{-\alpha} - 1} \right)$	$\alpha \in (-\infty, 0) \cup (0, +\infty)$

(2) Great likelihood estimation is used to obtain the estimates of the unknown parameters in the Copula model. Considering the general case, let the marginal distribution functions of the continuous random variables X and Y be $F(x; \theta_1)$ and $G(y; \theta_2)$, respectively, and the corresponding marginal density functions be $f(x; \theta_1)$ and $g(y; \theta_2)$, respectively, where θ_1 and θ_2 are the location parameters in the marginal distribution. Let the selected Copula distribution function be $C(u, v; \alpha)$, Copula density function $c(u, v; \alpha) = \frac{\partial^2 C(u, v; \alpha)}{\partial u \partial v}$, α denotes the unknown parameter in the Copula function. At this point the joint distribution function of (X, Y) can be written as:

$$H(x, y; \theta_1, \theta_2, \alpha) = C(F(x; \theta_1), G(y; \theta_2); \alpha) \quad (16)$$

The likelihood function of the sample $(X_i, Y_i, i = 1, 2, \dots, n)$ is

$$L(\theta_1, \theta_2, \alpha) = \prod_{i=1}^n c(F(x_i; \theta_1), G(y_i; \theta_2); \alpha) f(x_i; \theta_1) g(y_i; \theta_2) \quad (17)$$

The maximum likelihood estimates of the unknown parameters θ_1 , θ_2 and α in the marginal distribution and Copula function can be obtained by solving for the maximum points of the log-likelihood function.

$$\hat{\theta}_1, \hat{\theta}_2, \hat{\alpha} = \operatorname{argmax} \ln L(\theta_1, \theta_2, \alpha) \quad (18)$$

(3) Calculate the squared Euclidean distance d_{Gu} between the selected Copula model and the empirical Copula model. The smaller d_{Gu} indicates a better fit, so the model with the smallest d_{Gu} is selected as the optimal Copula model.

Let the samples $(x_i, y_i) (i = 1, 2, \dots, n)$ come from the two-dimensional overall (X, Y) , and the empirical distribution functions of X and Y are $F_n(x)$ and $G_n(y)$, the empirical Copula of the samples can be written as

$$\hat{C}_n(u, v) = \frac{1}{n} \sum_{i=1}^n I[F_n(x_i \leq u)] \cdot I[G_n(y_i \leq v)], \quad u, v \in [0, 1] \quad (19)$$

where $I[\cdot]$ is the indicative function, $I[F_n(x_i \leq u)] = 1$ when $F_n(x_i \leq u)$; otherwise $I[F_n(x_i \leq u)] = 0$.

Let the value of the joint Copula function of X and Y be $C(u_i, v_i)$, then the squared Euclidean distance can be obtained at this point.

$$d_{Gu} = \sum_{i=1}^n |\hat{C}_n(u_i, v_i) - C(u_i, v_i)|^2 \quad (20)$$

2.4.2 Reliability calculation considering multiple failure modes' correlation

There is a correlation between the various failure modes of mechanisms due to common loads and same working environment. Assuming that a component has n failure modes, the generalized performance function corresponding to a certain failure mode is

$$g_i(X_i) = \sigma_i - S_i = \begin{cases} \leq 0, & \text{failure state} \\ > 0, & \text{safe state} \end{cases} \quad (21)$$

where σ_i and S_i denote the generalized strength and stress of the component under this failure mode, respectively.

If there is a series relationship between the failure modes of the component, the reliability of the component can be expressed as:

$$R = P(g_1(X_1) > 0, g_2(X_2) > 0, \dots, g_n(X_n) > 0) = \int_0^\infty \int_0^\infty \dots \int_0^\infty f_G(g_1(x_1), g_2(x_2), \dots, g_n(x_n)) dg_1 dg_2 \dots dg_n \quad (22)$$

where f_G is the joint probability density function of $g_1(x_1), g_2(x_2), \dots, g_n(x_n)$.

There are two problems with the application of the above formula. One is that it is very difficult to determine the joint probability density function, and the other is that the method of calculating the reintegration is very complicated. Using Copula function can avoid these two problems. Suppose a mechanism has two failure modes. g_1 and g_2 are used to represent their corresponding performance functions. If the failure modes are connected in series, this means that the occurrence of any failure mode will cause the component to fail and the reliability of the component can be expressed as:

$$\begin{aligned} R &= P(g_1(X_1) > 0, g_2(X_2) > 0) \\ &= 1 - P(g_1(X_1) \leq 0) \\ &\quad - P(g_2(X_2) \leq 0) \\ &\quad + P(g_1(X_1) \leq 0, g_2(X_2)) \\ &= 1 - F_1(0) - F_2(0) \\ &\quad + F_{g_1g_2}(F_1(0), F_2(0)) \end{aligned} \quad (23)$$

where: $F_1(0)$ and $F_2(0)$ are the failure probabilities of each failure mode. F_1 and F_2 are the probability distribution functions of each failure mode. $F_{g_1g_2}$ is the joint distribution function of the two performance functions.

$$\begin{aligned} R &= 1 - F_1(0) - F_2(0) + C_{g_1g_2}(F_1(0), F_2(0)) \\ &= 1 - F_1(t) - F_2(t) \\ &\quad + C_{g_1g_2}(F_1(t), F_2(t)) \end{aligned} \quad (24)$$

Extending the case of two failure modes to n failure modes,

the reliability of the system can be expressed as:

$$\begin{aligned} R &= P(g_1(X_1) > 0, g_2(X_2) > 0, \dots, g_n(X_n) > 0) \\ &= 1 - \sum_{i=1}^n P(g_i(X) \leq 0) \\ &\quad + \sum_{1 \leq i_1 \leq i_2 \leq n} P(g_{i_1}(X) \leq 0, g_{i_2}(X) \leq 0) + \dots \\ &\quad + (-1)^k \sum_{1 \leq i_1 \leq i_2 \leq i_k \leq n} P(g_{i_1}(X) \leq 0, g_{i_2}(X) \leq 0, \dots, g_{i_k}(X) \leq 0) \\ &\quad + (-1)^n P(g_1(X) \leq 0, g_2(X) \leq 0, \dots, g_n(X) \leq 0) \\ &= 1 - \sum_{i=1}^n F_i(t) + \sum_{1 \leq i_1 \leq i_2 \leq n} C_{g_{i_1}g_{i_2}}(F_{i_1}(t), F_{i_2}(t)) + \dots \\ &\quad + (-1)^k \sum_{1 \leq i_1 \leq i_2 \leq i_k \leq n} C_{g_{i_1}g_{i_2} \dots g_{i_k}}(F_{i_1}(t), F_{i_2}(t), \dots, F_{i_k}(t)) \\ &\quad + (-1)^n C_{g_1g_2 \dots g_n}(F_1(t), F_2(t), \dots, F_n(t)) \end{aligned} \quad (25)$$

2.5 Kaplan-Meier estimation of experimental censored data

When analyzing the reliability of most mechanical products, censored data is the most prevalent reliability metric [1,3]. Kaplan-Meier estimation [7,11,25] is introduced in this paper to analyze the experimental censored data. Suppose there are w failures occurred during the timed end test, and the samples of failure data were arranged in ascending order as follows.

$$t_{(1)} \leq t_{(2)} \leq \dots \leq t_{(w)} \quad (26)$$

The failure probability based on Kaplan-Meier estimation is:

$$\begin{aligned} P(T_F > t_i) &= P(T_F > \delta t) \cdot P(T_F > t_{(1)} + \delta t | T_F > \\ &\quad \cdot P(T_F > t_{(2)} + \delta t | T_F > t_{(2)}) \dots \\ &\quad > t_{(i)} + \delta t | T_F > t_{(i)}) \end{aligned} \quad (27)$$

where δt is an arbitrarily small time interval with no failure data during the time interval. Therefore, the Kaplan-Meier estimate

of the reliability function based on censored data is

$$R(t) = \prod_{\text{all } i \text{ such that } t_{(i)} \leq t} \hat{P}_i = \prod_{\text{all } i \text{ such that } t_{(i)} \leq t} \frac{n_i}{n} \quad (28)$$

where n_i is the number of operational units right before $t_{(i)}$.

In order to calculate the confidence intervals for the Kaplan-Meier estimator, it is necessary to estimate its variance. The variance of Kaplan-Meier estimation can be obtained by Greenwood formula [13]:

$$\text{var}[\hat{R}(t_i)] = [\hat{R}(t_i)]^2 \sum_{j \leq i} \frac{m_j}{n_j(n_j - m_j)} \quad (29)$$

For Kaplan-Meier estimation, one of its maximum likelihood estimates or limit estimates has an approximate normality. Therefore, the role of a normal approximation is to adjust the confidence interval constructed near $\hat{R}(t_i)$. The confidence interval at 95 % confidence level is:

$$R_{95\%}(t_i) = \hat{R}(t_i) \pm 1.96\sigma(t_i) \quad (30)$$

3. Methodology implementation

3.1 Engineering problem description

A reliable rifle can be a deterrent, and therefore a tool that ensures peace and security. The firearm mainly transforms the chemical energy of gunpowder into mechanical kinetic energy of the automaton to complete the motion cycle of firing,

unlocking, recoiling, case ejecting, counter-recoiling, feeding and locking, etc. Compared with the general mechanism movement, it has the following characteristics: (1) the automaton completes intermittent reciprocating motion of variable mass and high frequency under high temperature and high pressure; (2) the mechanism movement relies on high-velocity impact to complete, and there are numerous failure modes with correlations; (3) the case throwing and cartridge pushing actions are completed in dynamic, not fully constrained conditions and are subject to external environment; (4) there will be a significant performance degradation of the counter-recoil spring, hammer spring, piston spring and other spring parts with the increase in firing circles. Consequently, the motion reliability of the firearm mechanism is a dynamic process that varies with firing circles, and the influence of environmental factors and the correlation between multiple failure modes also need to be considered in this process. Taking an air-guided automatic rifle product as the research object, based on its automatic cycle diagram, the motion of the automatic mechanism can be represented as the point-line diagram shown in Figure 2, where the line segment indicates the motion process and the node indicates the impact combination or impact separation.

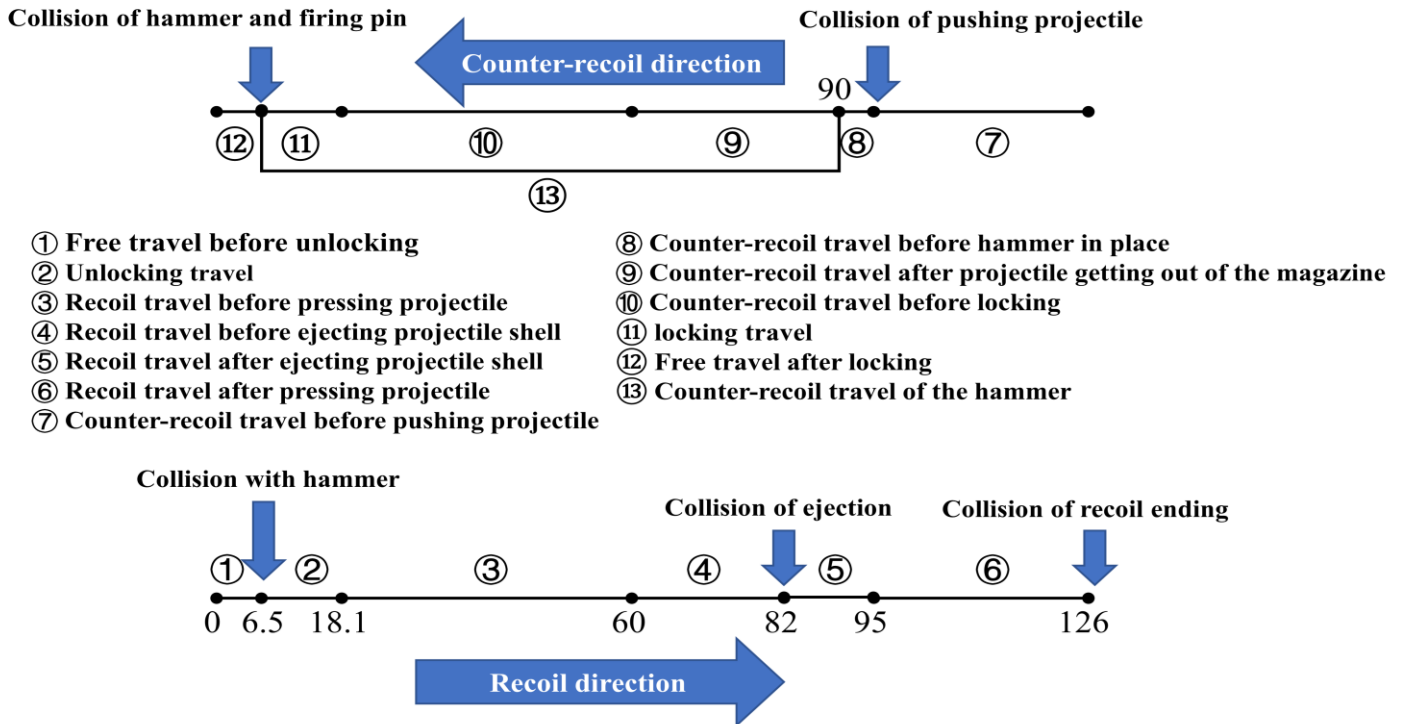


Fig.2. The point-line diagram of the motion of the automatic mechanism.

Since there are differences in the masses of moving parts corresponding to different stages of motion of the automaton and the magnitude of the combined forces applied, for this reason, the kinetic equations are divided into 13 stages based on the nodes, updating each parameter for the subsequent stage of motion. The equations for each stage can be expressed as

$$\mathbf{M}\ddot{x} = \mathbf{F} \quad (31)$$

where x denotes the displacement of the moving part, \mathbf{M} denotes the vector of the mass of the moving part corresponding to each stage, and \mathbf{F} denotes the vector of the magnitude of the combined force applied to each stage.

$$M = \begin{bmatrix} m_1 \\ m_1 + \frac{k_{tr1}^2}{\eta} m_3' + \frac{k_{tr2}^2}{\eta} m_3 \\ m_1 + m_2 + m_3 + m_5 \\ m_1 + m_2 + m_3 + m_5 \\ m_1 + m_2 + m_3 \\ m_1 + m_2 + m_3 \\ m_1 + m_2 + m_3 + m_4 \\ m_1 + m_3 + m_4 \\ m_1 + m_3 + m_4 \\ m_1 + \frac{k_{tr1}^2}{\eta} m_3' + \frac{k_{tr2}^2}{\eta} m_3 \\ m_1 \\ m_2 \end{bmatrix},$$

$$F = \begin{bmatrix} F_1 - k_1 x_1 + \mu m_1 g \\ F_1 - k_1 x_1 + \mu(m_1 + m_3)g + \frac{k_{tr1}}{\eta} F_{tr1} + \frac{k_{tr2}}{\eta} F_{tr2} \\ F_1 - k_1 x_1 + F_2 + k_2(d_0 - x_1) + \mu(m_1 + m_2 + m_3 + m_5)g \\ F_1 - k_1 x_1 + F_2 + k_2(d_0 - x_1) + \mu[F_0 - (m_1 + m_2 + m_3 + m_5)g] \\ F_1 - k_1 x_1 + F_2 + k_2(d_0 - x_1) + \mu[F_0 - (m_1 + m_2 + m_3)g] \\ F_1 - k_1 x_1 + F_2 + k_2(d_0 - x_1) + \mu(m_1 + m_2 + m_3)g \\ F_1 - k_1 x_1 + F_2 + k_2(d_0 - x_1) - \mu(m_1 + m_2 + m_3)g \\ F_1 - k_1 x_1 + F_2 + k_2(d_0 - x_1) - \mu[F_0 - (m_1 + m_2 + m_3 + m_4)g] \\ F_1 - k_1 x_1 + F_2 + k_2(d_0 - x_1) - \mu[F_0 - (m_1 + m_3 + m_5)g] \\ F_1 - k_1 x_1 - \mu(m_1 + m_3 + m_4)g \\ F_1 - k_1 x_1 - \mu(m_1 + m_3)g - \frac{k_{tr1}}{\eta} F_{tr1} - \frac{k_{tr2}}{\eta} F_{tr2} \\ F_1 - k_1 x_1 - \mu m_1 g \\ F_2 - k_2 x_2 - \mu m_2 g \end{bmatrix}$$

The meanings and values of the symbols in the equation are shown in Table 2.

Table 2. The meanings and values of the symbols in the equation

Symbols	Meanings	Units	Values (initial state)
m_1	Mass of bolt carrier	g	400
m_2	Mass of hammer	g	100
m_3	Mass of bolt	g	77
m_3'	Replacement mass of the bolt along its rotary axis	g	37
m_4	Mass of cartridge	g	12.5
m_5	Mass of case	g	6.5
x_1	Displacement of bolt carrier	mm	0

Symbols	Meanings	Units	Values (initial state)
x_2	Displacement of hammer	mm	6.5
μ	Friction coefficient between moving parts and receiver	-	0.265
F_0	Magazine spring force	N	20
F_1	Preload of counter-recoil spring	N	28
F_2	Preload of hammer spring	N	11
k_1	Stiffness of counter-recoil spring	N/m	240.6
k_2	Stiffness of hammer spring	N/m	90.5
k_{tr1}	Velocity transmission ratio along the rotation of bolt	-	0.81
k_{tr2}	Velocity transmission ratio along the translation of bolt	-	0.01
F_{tr1}	Resistance in the rotation of bolt	N	30
F_{tr2}	Resistance in the translation of bolt	N	1.05
η	Transmission efficiency of spiral groove	-	0.3
d_0	Distance between hammer and bolt carrier at the moment of firing	mm	7

3.2 Mechanism performance parameters and performance margin model

For the automaton motion mechanism, the main failure modes that cause the mechanism to stop firing are powerless striking, cartridge jam and case jam, accounting for more than 90 % of the total number of failures, and powerless striking, cartridge jam and case jam are directly related to the automaton motion velocity in the corresponding phase, so the striking velocity, cartridge-pushing velocity and case-ejecting velocity are determined as the mechanism performance parameters without considering the influence of other failure modes on the mechanism reliability. For the automaton motion mechanism, the performance parameter p with failure threshold p_{th} is a Lager-The-Better parameter, which indicates that the mechanism only fails when $p \leq p_{th}$. The failure thresholds for powerless striking, cartridge jam and case jam are generally determined by live-firing tests, and the values of the performance parameters and their failure thresholds taken in this paper are shown in Table 3.

Table 3. Values of the performance parameters and their failure thresholds.

Performance parameters	Units	Failure thresholds
striking velocity	m/s	4.2
cartridge-pushing velocity	m/s	2.6
case-ejecting velocity	m/s	3.5

The performance margin model of p can be written as:

$$m = \frac{p - p_{th}}{p} \quad (32)$$

where m is a dimensionless parameter, when the performance margin $m > 0$, the performance parameters will not exceed the failure threshold and the mechanism is reliable; when the performance margin $m < 0$, the performance parameters exceed the failure threshold and the mechanism is unreliable; when the performance margin $m = 0$, the performance parameters are equal to the failure threshold and the mechanism is in a critical state.

3.3 Temperature Influence on mechanism parameters

For piston-recoiled firearms, the direct source of the kinetic energy of the bolt carrier is the pressure in the gas chamber, and the change law of the powder gas pressure inside the gas chamber is related to the powder gas pressure inside the bore chamber. Therefore, the temperature change affects the bore pressure by influencing the burning rate of the powder, which in turn affects the initial energy of the automaton kinetic mechanism. The gas chamber pressure is calculated using the

empirical Bravin formula, and the velocity of the piston at any moment of free recoil can be written as an integral form of the gas chamber pressure load:

$$P_s = P_d e^{-\frac{t}{b}} (1 - e^{-\frac{t}{b}}) \quad (33)$$

$$v_t = \frac{S}{m_1} \int_0^t P_s dt \quad (34)$$

where P_s is the gas chamber pressure, P_d is the average pressure in the bore chamber at the instant when the cartridge nose passes through the gas port, α is the coefficient related to the structural parameters of the gas-operated device, b is the time coefficient related to the bore pressure impulse, S is the cross-sectional area of the piston, t is the operating time of gas chamber pressure, and v_t is the corresponding velocity of the bolt carrier.

The mapping relationship between the bore pressure and the initial conditions of the equation can be established through the Bravin empirical formula. The bore pressure curves at different temperatures measured during the test and the random distribution of the maximum bore pressure (fitted to a Gaussian distribution) are shown in Figure 3.

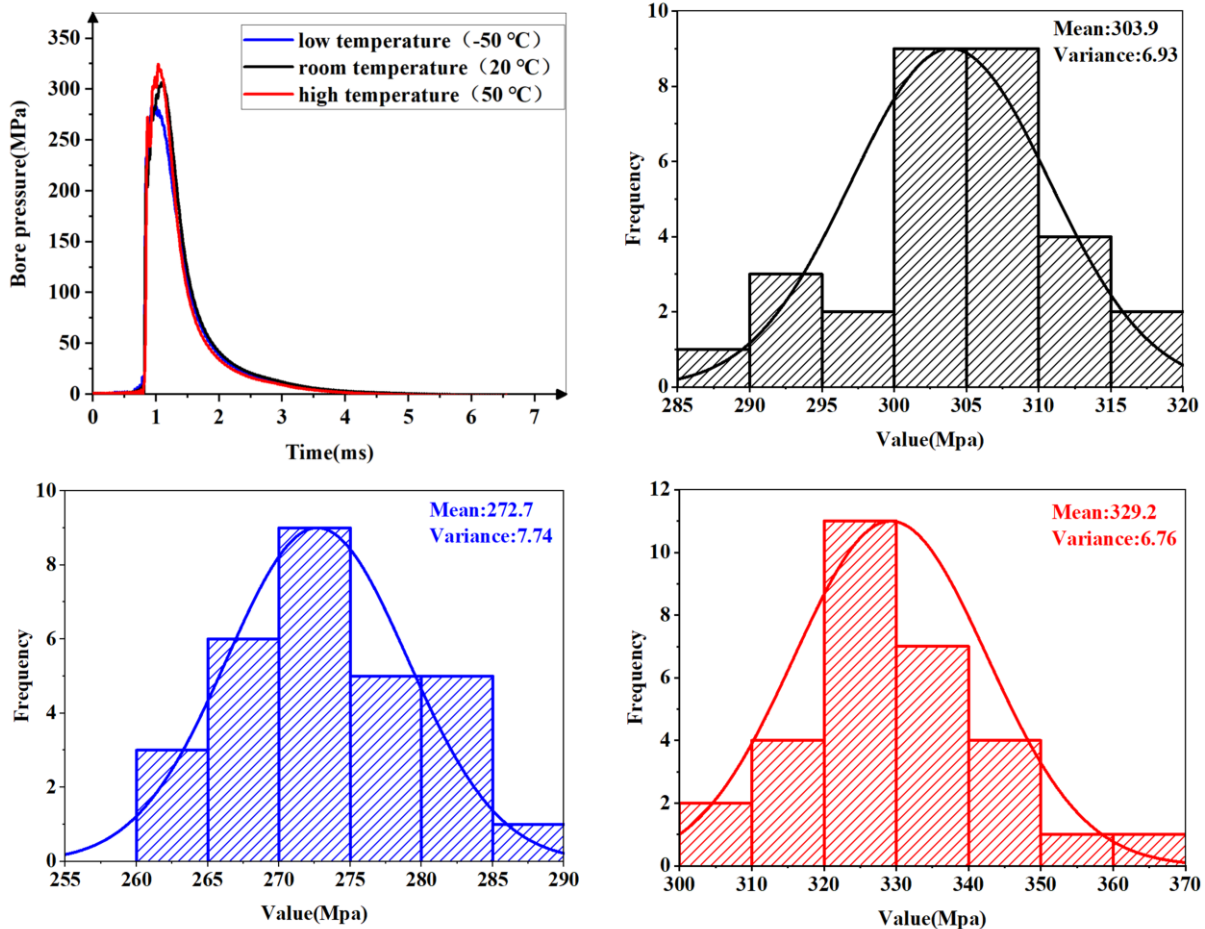


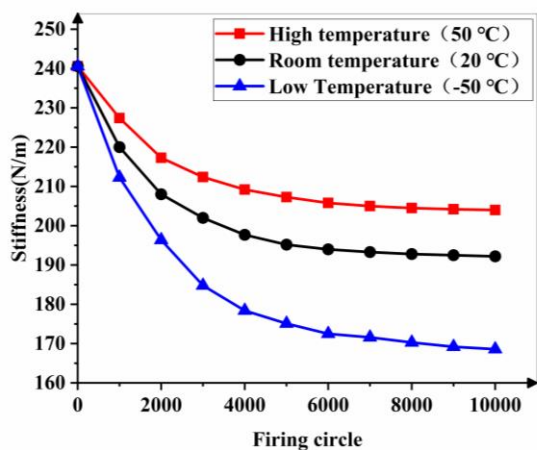
Fig.3. The bore pressure curves and the random distribution of the maximum bore pressure under different temperatures.

Based on the motion curves of the automaton measured at different temperatures, the random distribution of mechanism parameters, as shown in Table 4, were obtained by parameter identification under different temperatures.

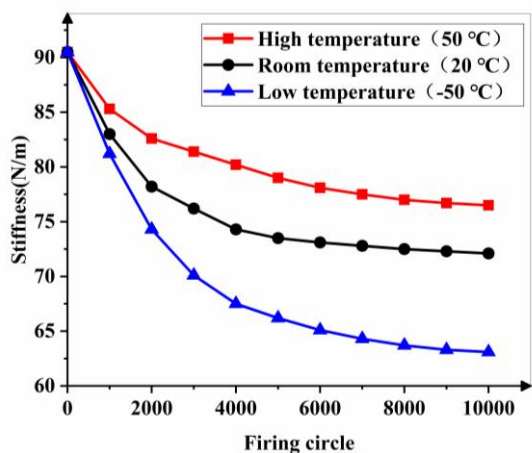
Table 4. The random distribution of mechanism parameters at different temperatures.

Parameters	Low temperature	Normal temperature	High temperature
Friction coefficient between moving parts and receiver Restitution	$N(0.15,0.12)$	$N(0.12,0.09)$	$N(0.16,0.13)$
coefficient for recoil ending impact	$N(0.45,0.23)$	$N(0.43,0.12)$	$N(0.43,0.14)$
Transmission ratio of hammer to pin impact	$N(0.96,0.1)$	$N(0.98,0.1)$	$N(0.98,0.1)$

During the environmental life test (10,000 rounds), the stiffness coefficients of the counter-recoil spring and hammer spring were measured and recorded every 1000 rounds, and the degradation path of springs with the firing circle under different temperatures was obtained as shown in Figure 4.



(a) Counter-recoil spring



(b) Hammer Spring.

Fig.4. The degradation path of springs with the firing circle under different temperatures.

3.4 The determination of optimal Copula model for dependent failure modes

Based on the historical experimental data of several automatic rifle products, the variation curves of the probability of the three failure modes with firing circles during the life cycle were obtained as shown in Figure 5.

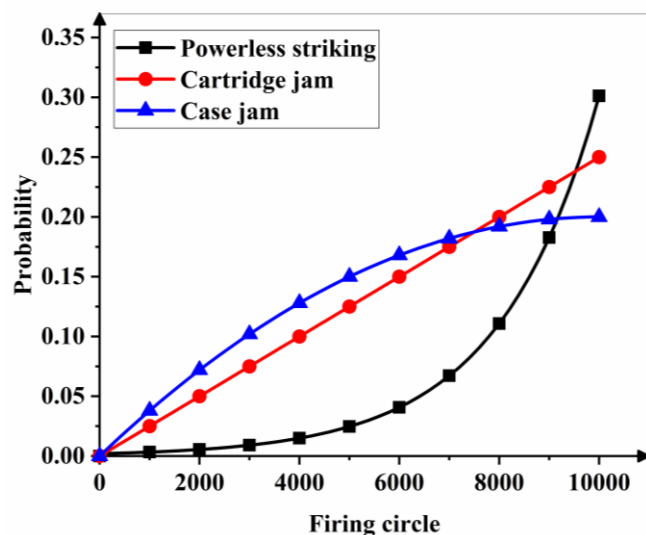
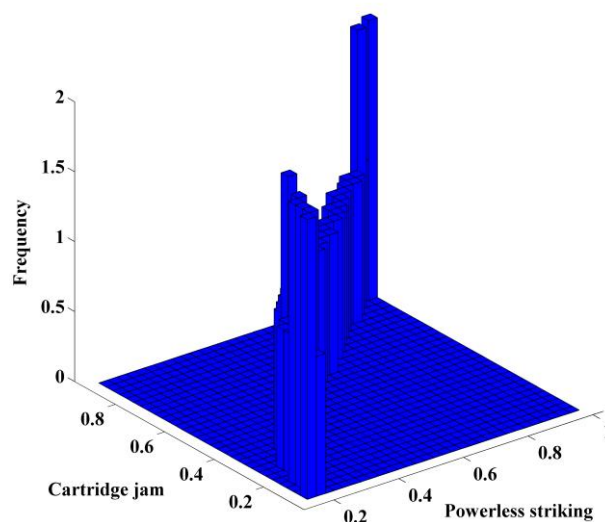
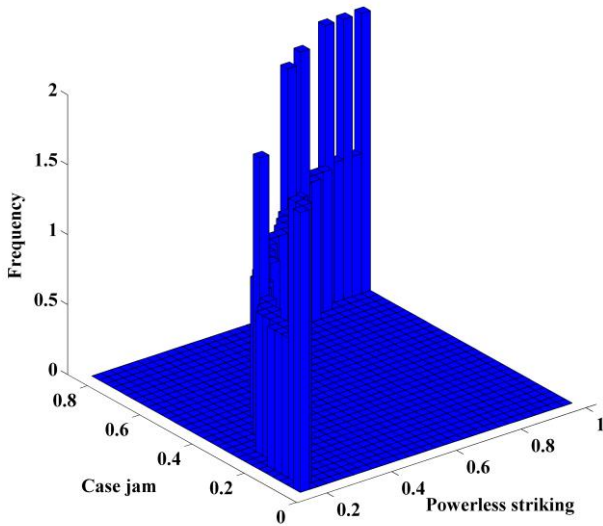


Fig.5. The variation curves of the probability of the three failure modes with firing circles.

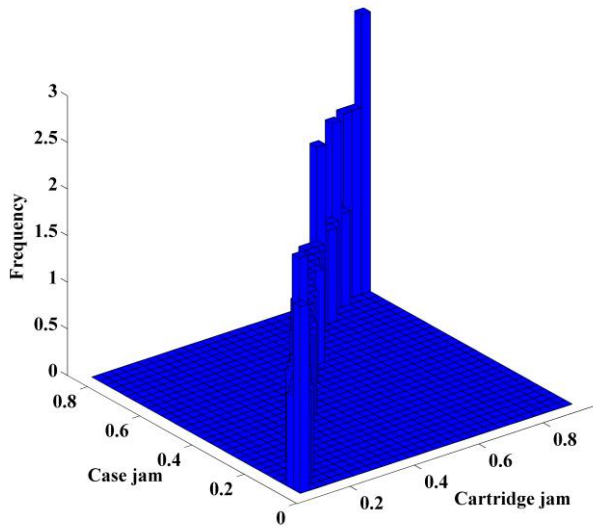
A bivariate frequency histogram of the failure rate is made based on the sampling of the curves in Figure 5 as shown in Figure 6.



(a) Powerless striking and cartridge jam



(b) Powerless striking and case jam



(c) Cartridge jam and case jam

Fig.6. A bivariate frequency histogram of the failure rate.

It can be seen that the frequency histogram has an essentially symmetric tail and a strong tail correlation, suggesting that the Copula density function describing this failure correlation likewise has a symmetric tail and a strong tail correlation. The binary Gaussian Copula function, the binary t-Copula function and the binary Frank Copula function are selected to describe the correlation between each failure mode, and the maximum likelihood estimation results of the unknown parameters and the squared Euclidean distances between the alternative Copula function and the empirical Copula function are shown in Table 5.

Table 5. The maximum likelihood estimation results of the unknown parameters and the squared Euclidean distances.

Failure modes	Gaussian Copula		t-Copula		Frank Copula	
	Parameter estimation results	squared Euclidean distance	Parameter estimation results	squared Euclidean distance	Parameter estimation results	squared Euclidean distance
Powerless striking, cartridge jam	0.9699	0.0450	0.9814	0.0267	38.9400	<u>0.0151</u>
Powerless striking, case jam	0.9154	0.1273	0.9486	0.0740	22.8509	<u>0.0416</u>
cartridge jam, case jam	0.9843	0.0235	0.9903	0.0139	52.6422	<u>0.0084</u>

According to the results in Table 5, the squared Euclidean distance between the Frank Copula function and the empirical Copula function is the smallest compared to Gaussian Copula and t-Copula, regardless of which two failure modes are correlated. This indicates that the Frank Copula function is most suitable for describing the correlation between failure modes of firearm mechanism, and its density function and distribution function are shown in Figure 7. The failure rate of various failure modes of general firearms products normally does not exceed 1 %. The correlation of the failure modes is strong when the failure rate is less than 1 %, which proves the necessity of considering the correlation of failure modes in reliability modelling.

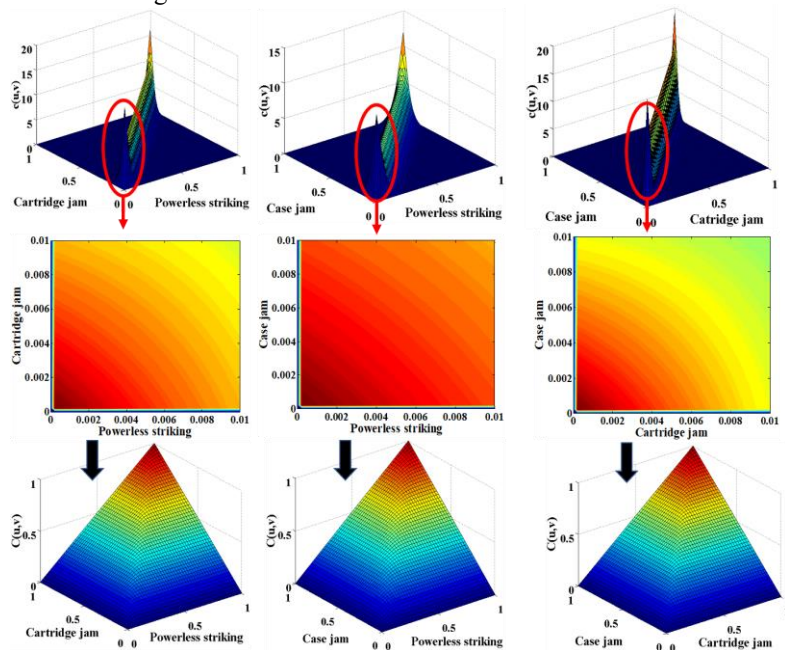
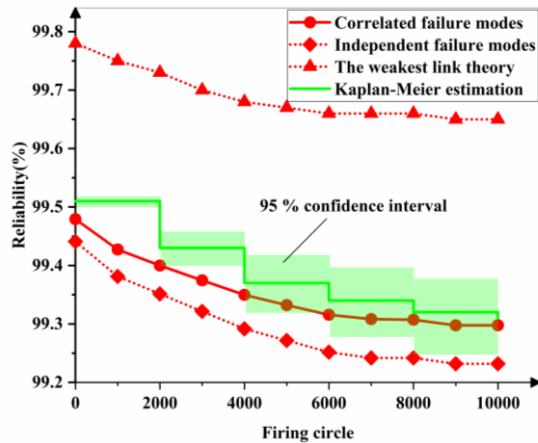


Fig.7. Density and distribution function of Frank Copula.

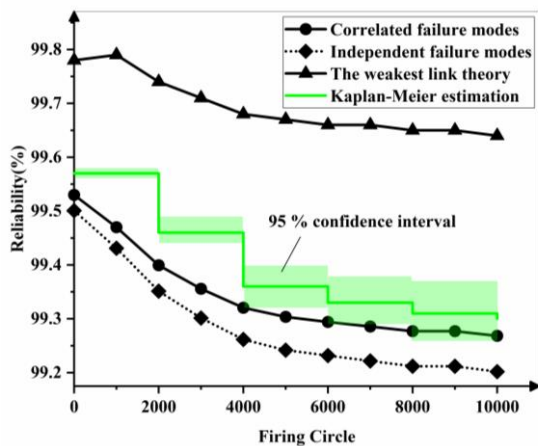
4. Results and discussion

4.1 Influence of failure modes' correlation on mechanism reliability

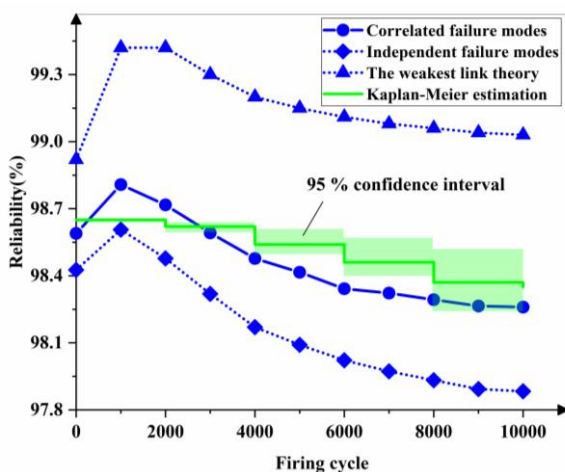
The following four types of data are compared and analyzed to obtain the mechanism reliability under different temperatures as shown in Figure 8.



(a) High temperature



(b) Room temperature



(c) Low temperature

Fig.8. The mechanism reliability under different temperatures.

The first type of reliability data: the reliability calculation results obtained by considering the failure modes' correlation; the second type of reliability data: the reliability calculation results obtained by not considering the failure modes' correlation. The third type of reliability data: the reliability calculation results based on the weakest link theory; the fourth type of reliability data: the variation of the mechanism reliability with firing circles using the Kaplan-Meier method based on censored data obtained from the environmental life experiment.

As can be seen in Figure 8, in the three temperature environments, the calculated reliability of the mechanism considering the failure modes' correlation is closer to the Kaplan-Meier estimation of the experimental data than that without considering the failure mode correlation, which is more appropriate to practical situation. In any condition, the reliability results obtained without considering the failure modes' correlation are lower than those obtained with considering the failure mode correlation, indicating the reliability of the mechanism tends to be underestimated without considering the failure modes' correlation. It is interesting that only at low temperature there is a peak at the beginning (for $n = 1000$) shown in Figure. 8(c). Since the variable is temperature, detailed explanation is given in Section 4.2.

According to the reliability boundary theory [9], the lower limit of system reliability is the reliability result obtained based on the independence assumption, whereas the upper limit of reliability is obtained from the weakest link theory, i.e., the system reliability is determined by the most prone failure mode. The reliability of the actual system ranges between the aforementioned upper and lower limits. The calculation results in Figure. 8 demonstrate that the reliability results obtained by considering the failure modes' correlation and the Kaplan-Meier estimation of the experimental censored data are between the lower limit of reliability obtained by the complete independence of failure modes and the upper limit of reliability obtained by the weakest link theory, which is in accordance with the general rule. This suggests that the Copula description based on failure mode correlation is valid and feasible in the reliability analysis of the mechanism with multiple failure modes.

4.2 Influence of environmental temperature on mechanism reliability

The calculated mechanism reliability under different ambient temperatures is shown in Figure 9.

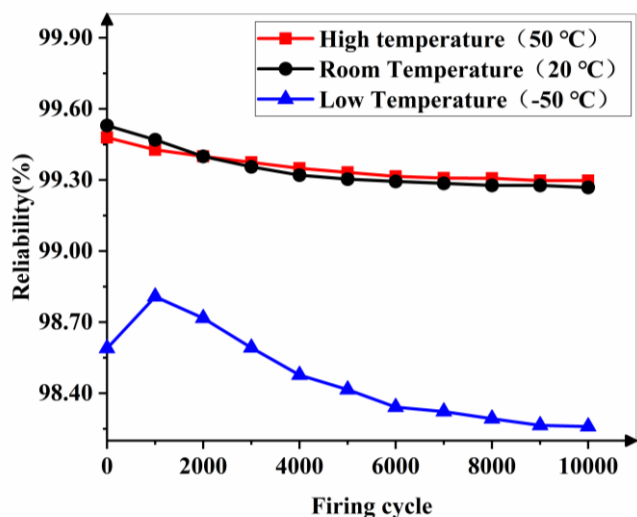


Fig.9. Reliability under different temperatures.

Overall, the reliability of the mechanism shows a decreasing trend with the increase of firing circles in the life range, which is influenced by the spring force degradation and random shock. The change of mechanism reliability in the high temperature environment is close to that in the normal ambient environment, while the effect of low temperature environment on mechanism reliability is more pronounced. The reliability at the end of life for normal, high and low temperature environments decreased by 0.263 %, 0.182 % and 0.335 %, respectively, compared to the initial state. The reliability of the mechanism at the initial state was highest for the normal environment, while the reliability of the mechanism at the end of life was highest for the high temperature environment and lowest for the low temperature environment during the whole life stage. Likewise, the log-rank test results of the Kaplan-Meier estimation of three temperature levels also indicate different outcomes have significant difference.

The aforementioned outcomes can be attributed to the "complementary effect" and "excitation effect" of the parameters. The "complementary effect" of the parameters refers to the fact that the initial energy of the automaton motion mechanism increases with the increase in bore pressure under high temperature environment, which is beneficial to the improvement of mechanism reliability. However, the mean

value of the friction coefficient increases, and the standard deviation of the impact coefficient of restitution increases, which is detrimental to the improvement of mechanism reliability. Therefore, from the aspect of enhancing mechanism reliability, there is a "complementary effect" between the parameters and the mechanism reliability does not decrease significantly. Likewise, the "excitation effect" of the parameters refers to the low temperature environment where the bore pressure decreases and the initial energy of the automaton motion mechanism decreases, which is not conducive to improving the mechanism reliability. However, at this time, the mean value of the friction coefficient increases, the standard deviation of the impact coefficient of restitution increases and the transmission ratio of the hammer striking the firing pin decreases, which are not conducive to improving the mechanism reliability. There is an "excitation effect" between the parameters, and the reliability of the mechanism decreases drastically.

In addition, although the mechanism reliability shows a decreasing trend in general, there is a phenomenon that the reliability increases momentarily at the beginning of the firing circles under low-temperature environment. The fundamental reason for this phenomenon is that the mechanism reliability is a comprehensive expression of the probability of various failure modes, and not all the failure modes have a higher failure rate as the firing circles increase. The variation of the failure rate of each failure mode with the firing circle under low temperature condition is shown in Figure 10.

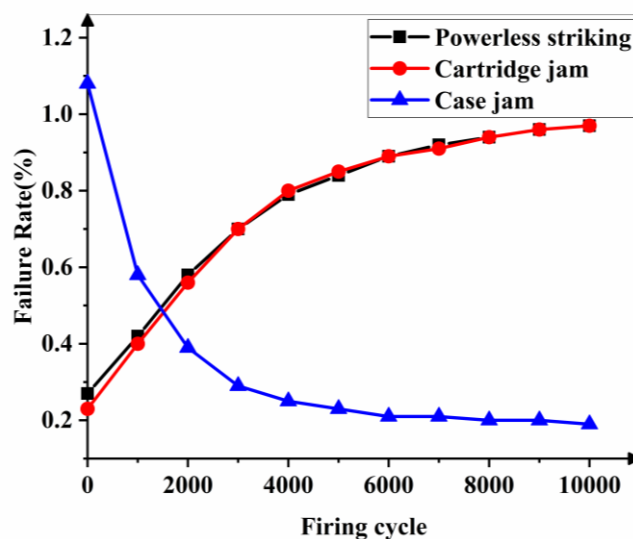


Fig.10. Failure rates under low temperature condition.

With the increase of firing circles, the failure rates of powerless striking and cartridge jam keep increasing and the failure rate of case jam keeps decreasing. In the early stage of firing circles, the performance of the counter-recoil spring and hammer spring degrade significantly, resulting in larger velocity in recoiling process and smaller velocity in recoiling and striking process, which is unfavorable for cartridge pushing and striking but favorable for case ejecting, and the failure rate of case jam decreases significantly, and the contribution to the improvement of reliability is greater than that of the improvement of failure rate of powerless striking and cartridge jam.

5. Conclusion

This paper proposes a mechanism reliability analysis method considering the influence of environmental factors and failure modes' correlation, by quantifying the influence of environmental factors by random distribution of parameters and degradation path, modelling multi-failure modes' correlation based on Copula function, calculating characteristic output parameters by discrete mechanism dynamics equation and obtaining dynamic changes of mechanism reliability by combining performance margin theory and failure criterion. The reliability modelling of an automatic mechanism of a firearm

Acknowledgements

The author(s) disclosed receipt of the following financial support for the research, authorship, and/or publication of this article: this paper is supported by Foundation Enhancement Program for National Defense Science (NO.2019-jcjq-zd-138-00).

References

1. Abba B, Wang H and Bakouch HS. A reliability and survival model for one and two failure modes system with applications to complete and censored datasets. *Reliability Engineering & System Safety* 2022; 223: 108460. <https://doi.org/10.1016/j.ress.2022.108460>.
2. Adumene S, Khan F, Adedigba S, et al. Offshore system safety and reliability considering microbial influenced multiple failure modes and their interdependencies. *Reliability Engineering & System Safety* 2021; 215:107862. <https://doi.org/10.1016/j.ress.2021.107862>.
3. Altındağ Ö and Aydoğdu H. Estimation of renewal function under progressively censored data and its applications. *Reliability Engineering & System Safety* 2021; 216: 107988. <https://doi.org/10.1016/j.ress.2021.107988>.
4. Barrera J, Cancela H and Moreno E. Topological optimization of reliable networks under dependent failures. *Operations Research Letters* 2015; 43: 132-136. <https://doi.org/10.1016/j.orl.2014.12.014>.
5. Brandhorst HW and Rodiek JA. Space solar array reliability: A study and recommendations. *Acta Astronautica* 2008; 63: 1233-1238. <https://doi.org/10.1016/j.actaastro.2008.05.010>.
6. Cherubini U, Luciano E, Vecchiato W. *Copula methods in finance*. 1st Editio. Ltd, UK: John Wiley & Sons; 2004. ISBN: 0470863447 (alk. paper). <https://doi.org/10.1002/9781118673331>
7. Durczak K, Selech J, Ekielski A, Żelaziński T, Waleński M, Witaszek K. Using the Kaplan–Meier Estimator to Assess the Reliability of Agricultural Machinery. *Agronomy*. 2022; 12(6):1364. <https://doi.org/10.3390/agronomy12061364>.

under high and low temperature conditions is used as an engineering example to implement the proposed method in the paper. The main conclusions obtained are as follows:

(1) Since the reliability of the mechanism is the comprehensive performance of each component of the mechanism, the degradation of system parameters due to environmental factors and increasing working cycles causes mechanism reliability to decrease in general, while the "coupling effect" and "excitation effect" between the parameters "coupling effect" and "excitation effect" between the parameters may lead to an increase in mechanism reliability temporarily.

(2) Failure mode correlation cannot be neglected in mechanism reliability modelling where multiple failure modes coexist, and the Copula function can not only flexibly and accurately model the mechanism failure mode correlation, but also alleviate the burden of multiple integration calculations caused by multiple failure modes.

(3) The reliability calculation results of the automaton motion mechanism in high and low temperature environments are close to the results of Kaplan-Meier estimation of the test history data, and they all fall within the upper and lower bounds specified by the reliability boundary theory, which illustrates the practicality and reasonableness of the proposed method.

8. Feng YS. The development of a theory of mechanism reliability. *Reliability Engineering & System Safety* 1993; 41: 95-99. [https://doi.org/10.1016/0951-8320\(93\)90020-Y](https://doi.org/10.1016/0951-8320(93)90020-Y).
9. Gu Y, Fan C and Liang L, et al. Reliability calculation method based on the Copula function for mechanical systems with dependent failure. *Annals of Operations Research* 2022; 311: 99-116. <https://doi.org/10.1007/s10479-019-03202-5>.
10. Guo, C, Wang W, Guo B, Peng R. Maintenance optimization for systems with dependent competing risks using a copula function. *Eksploatacja i Niezawodność: Maintenance and Reliability*, 2013, 15(1), 9–17. <http://ein.org.pl/sites/default/files/2013-01-02.pdf>
11. J.H. Saleh , J.F. Castet , *Spacecraft Reliability and Multi-State Failures: A Statistical Approach*, John Wiley & Sons, 2011. DOI:10.1002/9781119994077.
12. Jiang C, Zhang W and Han X. A Copula function-based evidence theory model for correlation analysis and corresponding structural reliability method. *Journal of Mechanical Engineering*, 2017; 53: 199-209. DOI: 10.3901/JME.2017.16.199.
13. Kalbfleisch, John D, Prentice, Ross L. (2002). [Wiley Series in Probability and Statistics] *The Statistical Analysis of Failure Time Data (Kalbfleisch/The Statistical)* || Introduction.1–30. <https://doi.org/10.1002/9781118032985.ch1>.
14. Kang R. *Belief reliability theory and methodology*. Beijing: National Defense Industry Press; 2020. DOI:10.1007/978-981-16-0823-0.
15. Lee SJ, Gilmore BJ. The determination of the probabilistic properties of velocities and accelerations in kinematic chains with uncertainty. *Journal of Mechanical Design* 1991;113(1):84–90. <https://doi.org/10.1115/1.2912755>.
16. Lee. SW, Han SW, Lee HS. Reliability evaluation of an oil cooler for a high-precision machining center. *International Journal of Precision Engineering and Manufacturing* 2007;8(3):50-3.
17. Li H, Wang P and Huang X, et al. Vine copula-based parametric sensitivity analysis of failure probability-based importance measure in the presence of multidimensional dependencies. *Reliability Engineering & System Safety* 2021; 215: 107898. <https://doi.org/10.1016/j.ress.2021.107898>.
18. Li X, Liu Y and Chen C, et al. A copula-based reliability modelling for nonrepairable multi-state k-out-of-n systems with dependent components. *Proc IMechE, Part O: J Risk and Reliability* 2016; 230: 133-146. DOI: 10.1177/1748006X15596086.
19. Lin Q, Hong N, Jie R, et al. Investigation on design and reliability analysis of a new deployable and lockable mechanism. *Acta Astronautica* 2012, 73(Apr.-May):183–192. <https://doi.org/10.1016/j.actaastro.2011.12.004>.
20. Liu TS and Wang JD. A reliability approach to evaluating robot accuracy performance. *Mechanism and Machine Theory* 1994; 29: 83-94. [https://doi.org/10.1016/0094-114X\(94\)90022-1](https://doi.org/10.1016/0094-114X(94)90022-1).
21. [21] Lu H and Zhu Z. A method for estimating the reliability of structural systems with moment-matching and copula concept. *Mechanics Based Design of Structures and Machines* 2018; 46: 196-208. <https://doi.org/10.1080/15397734.2017.1324312>.
22. Mahdi Tavangar, Marzieh Hashemi. Reliability and maintenance analysis of coherent systems subject to aging and environmental shocks. *Reliability Engineering & System Safety* 2021; 218(5):108170. <https://doi.org/10.1016/j.ress.2021.108170>.
23. Nelsen, R. B. (2006). *An introduction to Copulas*. New York: Springer. DOI: 10.2307/1271100.
24. Rafiee K, Feng Q, Coit D W. Reliability assessment of competing risks with generalized mixed shock models. *Reliability Engineering & System Safety* 2017; 159(MAR.):1-11. <https://doi.org/10.1016/j.ress.2016.10.006>.
25. Ragab A, Ouali M and Yacout S, et al. Remaining useful life prediction using prognostic methodology based on logical analysis of data and Kaplan-Meier estimation. *Journal of Intelligent Manufacturing* 2016; 27: 943-958. <https://doi.org/10.1007/s10845-014-0926-3>.
26. Shen J, Elwany A and Cui L. Reliability analysis for multi-component systems with degradation interaction and categorized shocks. *Applied Mathematical Modelling* 2018; 56: 487-500. <https://doi.org/10.1016/j.apm.2017.12.001>.
27. Stern R E, Song J, Work D B. Accelerated Monte Carlo system reliability analysis through machine-learning-based surrogate models of network connectivity. *Reliability Engineering & System Safety* 2017; 164:1-9. <https://doi.org/10.1016/j.ress.2017.01.021>.
28. Voit M. *Hubble Space Telescope: New Views of the Universe*. 1st ed. USA: Harry N. Abrams; 2000.
29. Wu JN, Yan SZ and Li J, et al. Mechanism reliability of bistable compliant mechanisms considering degradation and uncertainties: Modelling and evaluation method. *Applied Mathematical Modelling* 2016; 40: 10377-10388. <https://doi.org/10.1016/j.apm.2016.07.006>.
30. Wu JN, Yan SZ and Zuo MJ. Evaluating the reliability of multi-body mechanisms: A method considering the uncertainties of dynamic performance. *Reliability Engineering & System Safety* 2016; 149: 96-106. <https://doi.org/10.1016/j.ress.2015.12.013>.
31. Wu JN, Yan SZ, Xie LY. Reliability analysis method of a solar array by using fault tree analysis and fuzzy reasoning Petri net. *Acta*

- Astronautica 2011;69(11):960–8. <https://doi.org/10.1016/j.actaastro.2011.07.012>.
32. Wu Z, Chen J, Wen B. A New Narrow-Bound Method for Computing System Failure Probability. In: GeoShanghai International Conference 2006. DOI:10.1061/40865(197)12.
 33. X Huang, S Jin, X He, D He. Reliability analysis of coherent systems subject to internal failures and external shocks. Reliability Engineering & System Safety 2019; 181:75-83. <https://doi.org/10.1016/j.res.2018.09.003>.
 34. Yu S, Wang Z and Meng D. Time-variant reliability assessment for multiple failure modes and temporal parameters. Structural and Multidisciplinary Optimization 2018; 58: 1705-1717. <https://doi.org/10.1007/s00158-018-1993-4>.
 35. Zhang C, Wang L and Bai X, et al. Bayesian reliability analysis for copula based step-stress partially accelerated dependent competing risks model. Reliability Engineering & System Safety 2022; 227: 108718. <https://doi.org/10.1016/j.res.2022.108718>.
 36. Zhang D, Han X. Kinematic Reliability Analysis of Robotic Manipulator.pdf. Journal of Mechanical Design 2019; 142(4):1. <https://doi.org/10.1115/1.4044436>.
 37. Zheng H, Kong X and Xu H, et al. Reliability analysis of products based on proportional hazard model with degradation trend and environmental factor. Reliability Engineering & System Safety 2021; 216: 107964. <https://doi.org/10.1016/j.res.2021.107964>.
 38. Zhang J, Zhang Q and Kang R. Reliability is a science: A philosophical analysis of its validity. Applied Stochastic Models in Business and Industry 2018; 35: 275-277. <https://doi.org/10.1002/asmb.2426>.